Ocean and Coastal Management 163 (2018) 478–484

Contents lists available at ScienceDirect

Ocean and Coastal Management

journal homepage: www.elsevier.com/locate/ocecoaman

Puerto Rico sea level trend in regional context

Mark R. Jury[a,b,*]

[a] Physics Dept, Univ of Puerto Rico, Mayagüez, PR, 00681, USA
[b] Geography Dept, Univ of Zululand, KwaDlangezwa, 3886, South Africa

ARTICLE INFO

Keywords:
Climate change
Sea level rise
Puerto Rico
Beach erosion

ABSTRACT

Sea level (SL) is rising in Puerto Rico due to regional influences from weaker trade winds, in addition to global influences of thermal expansion and polar ice melt. The linear increase of SL has steepened in recent decades from +0.175 to +0.725 cm/yr. The faster rate of SL rise is partly attributed to diminishing ice volume (r = −0.80), notwithstanding a recent decline in the Atlantic Multi-decadal Oscillation. A sophisticated point-to-field regression analysis (N = 5980) demonstrates that daily fluctuations of SL in Puerto Rico are significantly enhanced by locally warmer sea temperatures via reduced evaporation, and correspond with lower air pressure accompanying late summer storms. These features point to regional air-sea interactions that affect SL rise over and above the background global signal. Extrapolating these trends, a rise of more than 0.3 m is expected by 2050.

1. Introduction

Coastal zones are dynamic and productive, but susceptible to erosion from rising sea level (SL) (Potter, 1996; Clark, 1997; Huang, 1997; Klein and Nicholls, 1999), especially Caribbean islands with their diminutive size and dense population (184 persons/km^2, IPCC, 2007; United Nations, 2016) and reliance on marine resources (Nicholls, 1998; IPCC, 2013). The Caribbean Sea is framed by South and Central America, the chain of Antilles Islands, and Atlantic Ocean. The island of Puerto Rico is centrally positioned (18ºN, 66ºW) and experiences steady trade winds and temperatures, and has a deep ocean thermocline (Murphy et al., 1999; Andrade and Barton, 2000). Atlantic water infiltrates the Caribbean Sea through the southeastern Antilles (Johns et al., 2002; Gyory et al., 2005), bearing fresh water from South American rivers. Currents flow westward ~0.5 m/s in latitudes 13-17ºN, eventually joining the Gulf Stream (Hernandez-Guerra and Joyce, 2000; Fratantoni, 2001; Johns et al., 2002; Wajsowicz, 2002).

While Caribbean climate processes and fluctuations have been revealed (Alvera-Azcárate et al., 2009), regional influences on SL trends are less informed. The effects of rising greenhouse gas emissions and warming temperatures may be compounded by local trends in the atmospheric circulation (IPCC, 2013; Jury, 2015). Reconstructed global SL records show a 0.19 cm/yr rate of rise in the 20th century (Church and White, 2011; Hamlington et al., 2011). As anthropogenic climate change accelerates the SL trend (Kenigson and Han, 2014), regional variations arise from the underlying geology, changes in the ocean thermohaline circulation (Yin et al., 2009; Hu et al., 2011; Boon, 2012; Ezer and Corlett, 2012; Sallenger et al., 2012; Ezer et al., 2013; Kopp, 2013), coupled low-frequency climate oscillations (Chambers et al., 2012; Liu, 2012; Booth et al., 2012; Scafetta, 2013; Zhang et al., 2013; Knudsen et al., 2014), and the artificial dependence of trend on record length (Baart et al., 2011). This work seeks to identify the factors underlying local SL rise, and is motivated by aerial surveys in Puerto Rico that reveal a ~1 m/yr narrowing of sandy beaches in recent decades (Thieler et al., 2007), The over-topping of dunes and inundation of aquifers will harm infrastructure, water supplies and tourism revenue ($50 B, Turner, 2015).

2. Data and methods

The SL is analyzed using quality controlled daily harbour measurements from National Oceanic and Atmospheric Administration (NOAA) gauges at San Juan 18.46°N, 66.12°W and Parguera 17.97°N, 67.05°W (PSMSL, 2013) on the northeast and southwest coast of Puerto Rico, respectively (Fig. 1a). The two time series are averaged to create a single record from 1955 to 2015 with < 1% missing data (mainly Jun 88 – Feb 89). Monthly averages are calculated and a low pass polynomial filter (Cleveland and Devlin, 1988, Trouet and VanOldenborgh, 2013) is applied to remove periods ≤ 12 months and fill gaps. SL trends are estimated by least squares regression within MS-excel, using default 1st and 2nd order schemes. Wavelet spectral energy is calculated in the two SL records at periods of multi-day and multi-year.

* Physics Dept, Univ of Puerto Rico, Mayagüez, PR, 00681, USA.
E-mail address: mark.jury@upr.edu.

https://doi.org/10.1016/j.ocecoaman.2018.08.006
Received 31 March 2018; Received in revised form 23 April 2018; Accepted 1 August 2018
Available online 04 August 2018

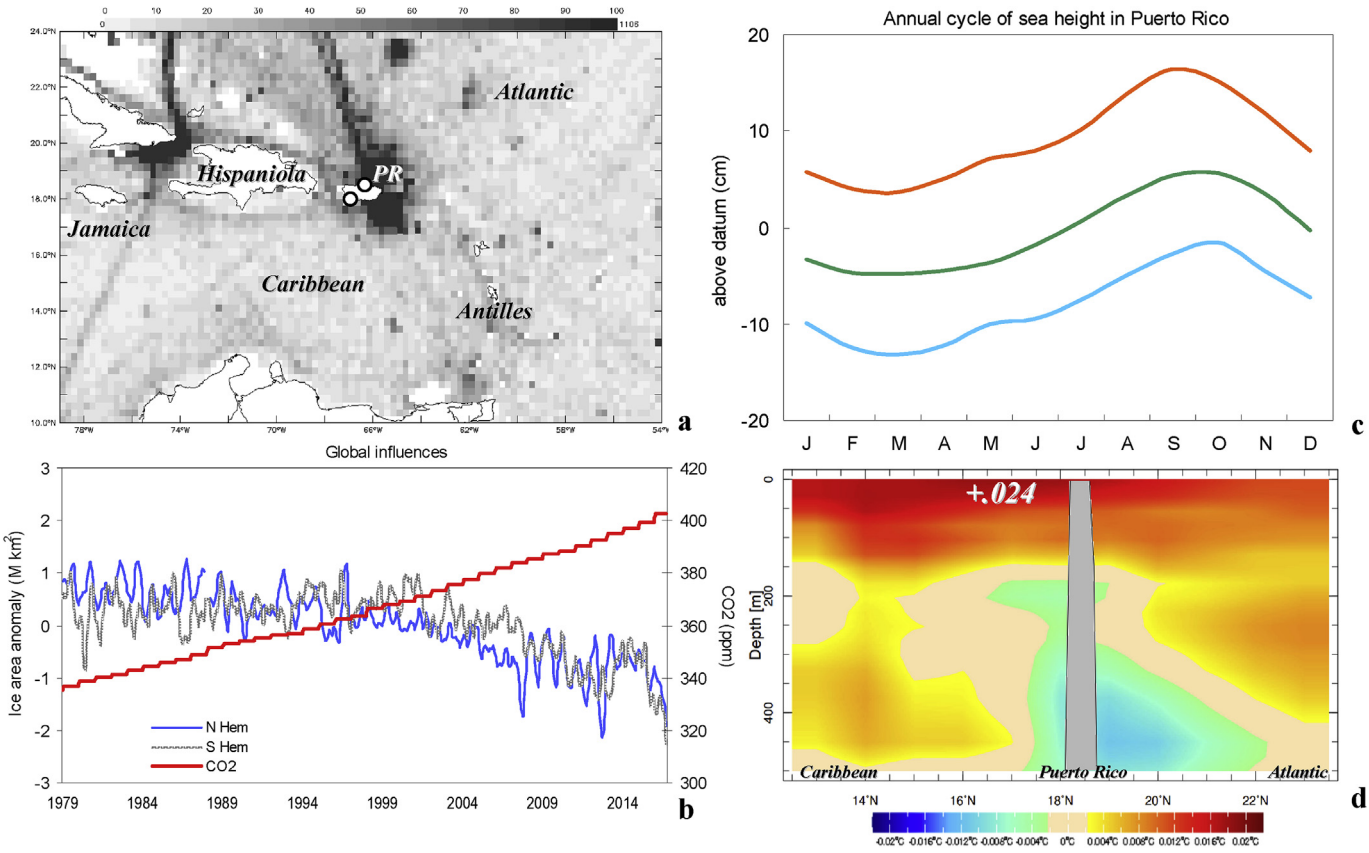

Fig. 1. (a) Ship reporting density for sub-surface temperature, with daily-monthly SL gauges (open dots) on the coast of Puerto Rico (PR). (b) Globally averaged annual CO2 concentration record and satellite-derived anomaly of (northern and southern) polar ice area (IPCC, 2013). (c) Mean annual cycle of SL with upper/lower 2.5% occurence. (d) Linear trend in subsurface ocean temperature averaged 64–68W from GODAS and SODA3 reanalysis; with Puerto Rico shaded.

Sea temperature warming in the Caribbean (10–24°N, 79-54°W) is analyzed over a depth section averaged 64°-68°W. The raw daily and filtered SL records are regressed onto field data on: sea surface height, outgoing longwave radiation (OLR) and sea surface temperature (SST) from satellite (Lee et al., 2007; Reynolds et al., 2007); and sea level pressure (SLP), sea surface temperature (SST), salinity, winds, and evaporation from ocean and atmosphere reanalyses: GODAS/SODA3 (Penny et al., 2015) and MERRA2 (Rienecker et al. 2011; Molod et al., 2015). Fig. 1a illustrates the data density underpinning these reanalyses (from WOA, 2013). The raw daily point-to-field correlations span the scatterometer era 1999–2015 (N = 5980), whereas the 12-month filtered SL correlations cover the satellite-reanalysis era 1980–2015 (N = 482). Serial auto-correlation and filtering reduce the degrees of freedom by a factor of ~10. The filtered SL record was regressed onto a variety of climate indices 1955+ (eg. Pacific Nino3 SST) and onto climate change variables 1980+ (eg. NSIDC polar ice, NODC ocean heat content, CDIAC global CO2 concentration).

Future SL projections to 2050, using the rcp8 scenario (VanVuuren et al. 2011), derive from CMIP-5 Hadley Centre v2 earth system model simulation (Collins et al. 2011) that corresponds with recent SL trends observed in Puerto Rico. Other CMIP-5 simulations show less agreement, for obscure reasons that could relate to feedback between over-land polar ice melt and rising greenhouse gas concentrations amongst other factors.

3. Results

3.1. Global context

Global influences on SL include thermal expansion and (over-land) ice melt, driven by rising greenhouse gases such as CO2, whose concentration is plotted together with satellite measurements of polar ice area in Fig. 1b. In the absence of geological uplift or subsidence, station records should follow the background global trends. The filtered PR SL time series correlates as follows: −0.37 with NSIDC N. Hem ice area, −0.30 with NSIDC S. Hem ice area, 0.45 with global CO2, -0.80 with NSIDC N. Hem ice volume (cf. Fig. 2d), and 0.42 with NODC global upper ocean (0–700 m) heat content in the period 1980–2015. The correlation with ice volume over Greenland is particularly striking, and indicates that global forces tend to override regional effects. In addition, the Atlantic Multi-decadal Oscillation has shown a decline since 2005 (Frajka-Williams et al., 2017) while PR SL has risen more steeply.

3.2. Annual cycle and section trend

The mean annual cycle of Puerto Rico SL peaks in September–October (Fig. 1c) when SLP is lowest. The SL follows the annual cycle of SST, rising in October and falling in March. These points tend to confirm known thermodynamic/hydrostatic influences, while steric effects tend to be most noteable at shorter time-scales (cf. section 3.4).

Trends in two ocean reanalysis (GODAS, SODA3) averaged over a depth section 64–68W 1980–2015 are illustrated in Fig. 1d. The sub-surface temperature trends show considerable warming (> +0.02 °C/yr) in the upper 100 m, and weak cooling below 200 m to the north of Puerto Rico. Westward currents have weakened in Caribbean 16-17°N (not shown), and the longer residence times for the build-up of surplus heat emerge in the upper layer warming of sea temperatures.

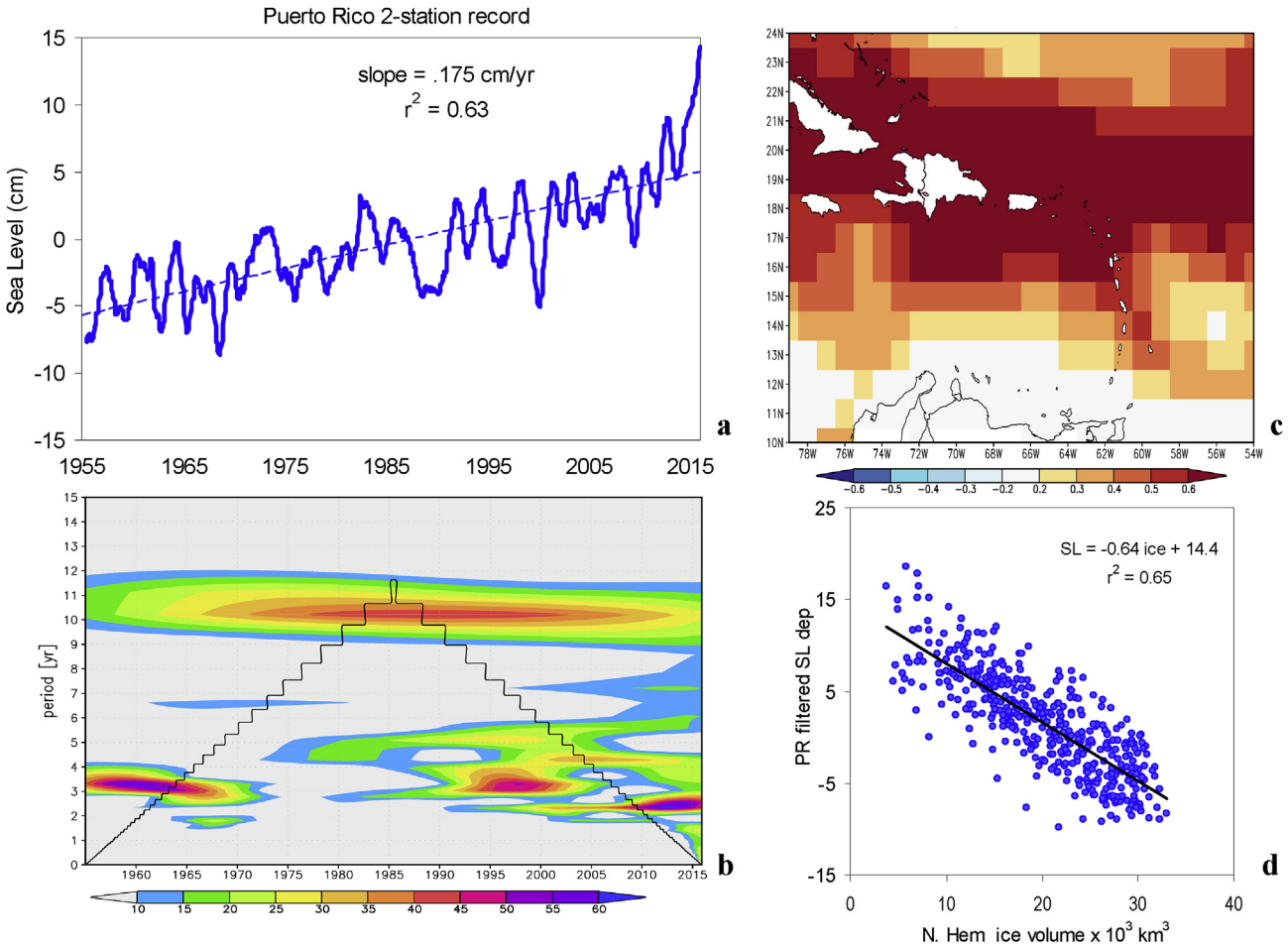

Fig. 2. (a) Time series and trend of 12-month filtered SL at Puerto Rico, and (b) wavelet spectra analysis (cone of validity outlined). (c) Regression of filtered SL record onto satellite altimeter-estimated sea surface height fields since 1992 (correlation fraction, N = 288). (d) Scatterplot of N. Hemisphere ice volume vs filtered SL 1980+.

3.3. Filtered SL trends and influences

The linear slope of 12-month filtered SL is 0.175 cm/yr since 1955 (Fig. 2a). The slope steepens to 0.725 cm/yr since 2005, a 4-fold increase consistent with Alfonso-Sosa (2016). Fluctuations in SL, represented by wavelet spectral analysis (Fig. 2b), show periods of 3 yr and 10 yr that are weakly associated with Pacific ENSO via Nino3 SST (r = 0.33, N = 724). The linear trend since 1955 accounts for 63% of variance (after filtering), while the 2nd order trend: $2^{-5}(t)^2 + 0.0012(t)$, covers 66% of variance (t = months). There is no significant spectral periodicity above 12 years in the Puerto Rico SL record (cf. Fig. 2b). Hence low frequency forcing (eg. Chambers et al., 2012) is minimal within the 60 yr time domain.

The point-to-field regression map for satellite sea surface height is extensive in the E-W axis but narrow N-S (Fig. 2c). While SL changes along the South American coast are unrelated, Puerto Rico's SL fluctuations and trends are shared with Jamaica, Hispanola and the northeastern Antilles Islands. Hence results may be extrapolated zonally with some confidence.

Point-to-field regression maps identify regional influences on SL rise in Puerto Rico (Fig. 3). Warmer sea temperatures and weaker trade winds reach significant values (Fig. 3a,c). Anticyclonic wind stress curl (Fig. 3f) encourages a deepening of the thermocline (20 °C isotherm, Fig. 3d). Fresher waters support higher SL (Fig. 3b) and suggest advancing river plumes. Fluctuations appear related to Pacific ENSO, wherein warm phase causes a southward shift of trade winds and higher SL. This corresponds with increased cloudiness over the tropical Pacific and decreased cloudiness over the Atlantic, as evident in the satellite OLR dipole pattern (Fig. 3g) and its local reflection (in SLP, Fig. 3b). The Hadley2 model projection of SL with rcp8 scenario (Fig. 3h) shows a rise of 0.87 cm/yr to 2050. The rate of SL rise appears insensitive to CO2 scenario (eg. similar trend for rcp4) and is consistent with observed SL trends since 2005 (0.725 cm/yr). Uncertainty in the projections naturally grows with time and is dependent on future greenhouse gas emissions and global to regional responses thereto.

3.4. Daily SL trends and fluctuations

While climate change induces a gradual rise of SL, coastal erosion is driven by daily spikes in SL associated with passing storms in late summer (Fig. 4a). Fitting a linear trend to the raw daily SL record since 1980, 13% of variance is explained by $+0.0007(t)$; fitting a 2nd order trend covers 16% of variance by $9^{-8}(t^2) - 0.00006(t)$, with t = days. Spectral energy at periods of 3–9 days (Fig. 4b) corresponds with the

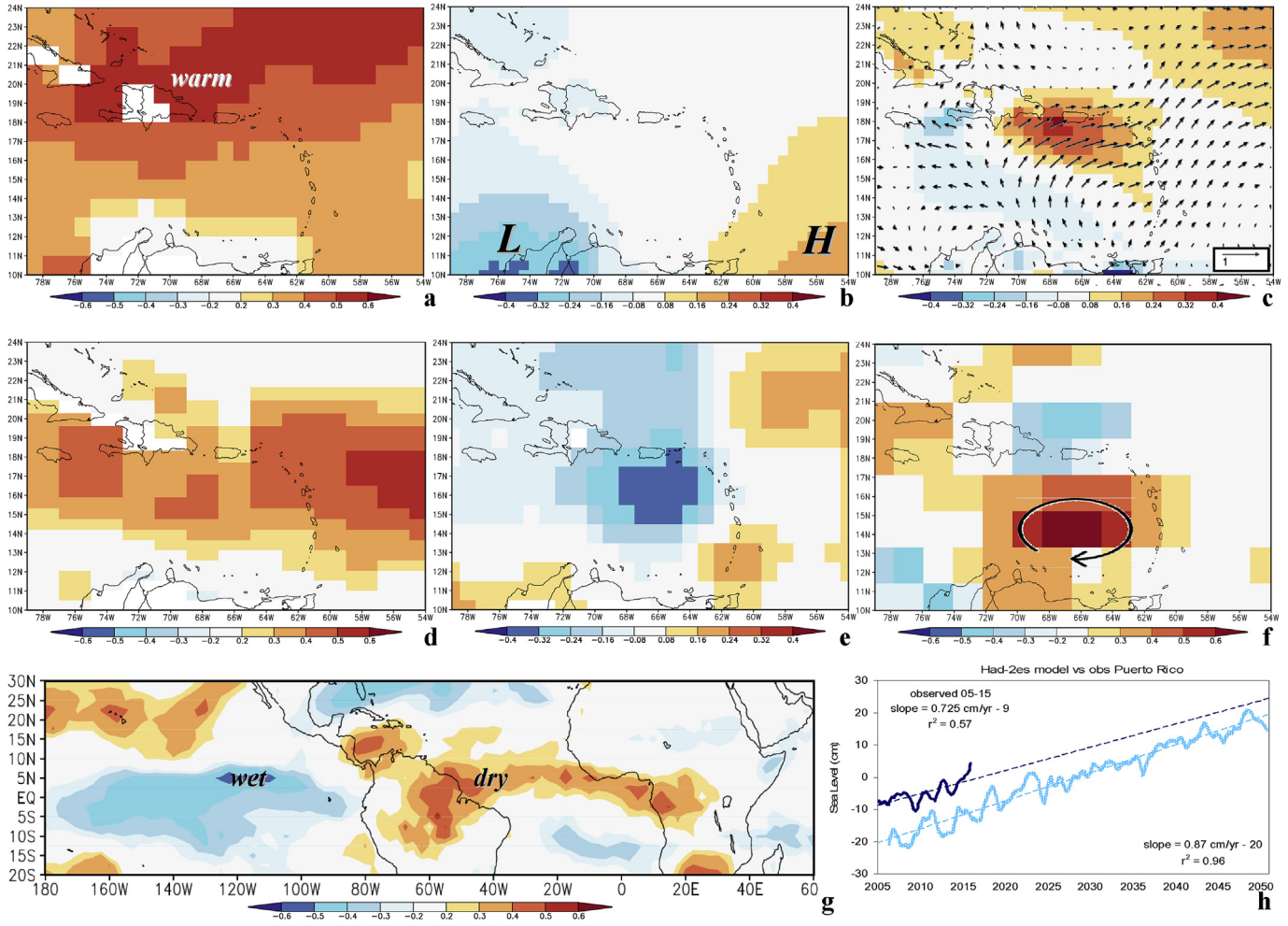

Fig. 3. Regression of 12-month filtered SL record 1980–2015 onto fields of: (a) SST, (b) SLP, (c) zonal wind (shading) and total wind vector, (d) depth of 20C isotherm, (e) sea surface salinity, (f) wind stress curl (+ = anticyclonic); (correlation fraction, N = 432). (g) Tropical hemispheric regression map of 12-month filtered SL record with detrended satellite OLR. (h) Projected SL trends with Hadley2 model under rcp8 scenario, compared with observed SL record starting in 2005, both 12-month filtered.

passage of easterly and westerly storms. The SLP-SL steric effect emerges from the scatterplot (Fig. 4c), with r^2 = 24%. Daily point-to-field regression maps (Fig. 4d–f) feature warmer sea temperatures (to the north) via reduced evaporation (to the south) and a cell of lower SLP. These features point to regional air-sea interactions that affect SL rise over and above the background global signal.

4. Conclusions

The sea level is rising in Puerto Rico due to regional effects of warmer SST, weaker evaporation/lower salinity, and declining SLP, in addition to the global influences of thermal expansion and polar ice melt. The rate of SL rise has steepened 4-fold in recent decades, from 0.175 to 0.725 cm/yr partly due to diminishing ice volume (cf. Fig. 2d, r −0.80), notwithstanding a declining Atlantic Multi-decadal Oscillation. Extrapolating these trends and considering the Hadley2 model results; a rise of 0.3 m is expected by 2050. With beach erosion inevitable (cf. Appendix, Caricoos, 2018), adaptation measures are needed. In the short-term, engineering works could be used to sustain coastal infrastructure and tourism in key places such as harbors and hotels. Puerto Rico does not have sufficient property tax revenue for beach sand reclamation. In the long-term, a planned retreat from the coast will require future development to be set back horizontally to achieve an elevation above ~3 m. Diversifying to renewable energy sources will enable Puerto Rico to join global mitigation efforts. On-going research will evaluate whether the accelerating trend of SL is sustained.

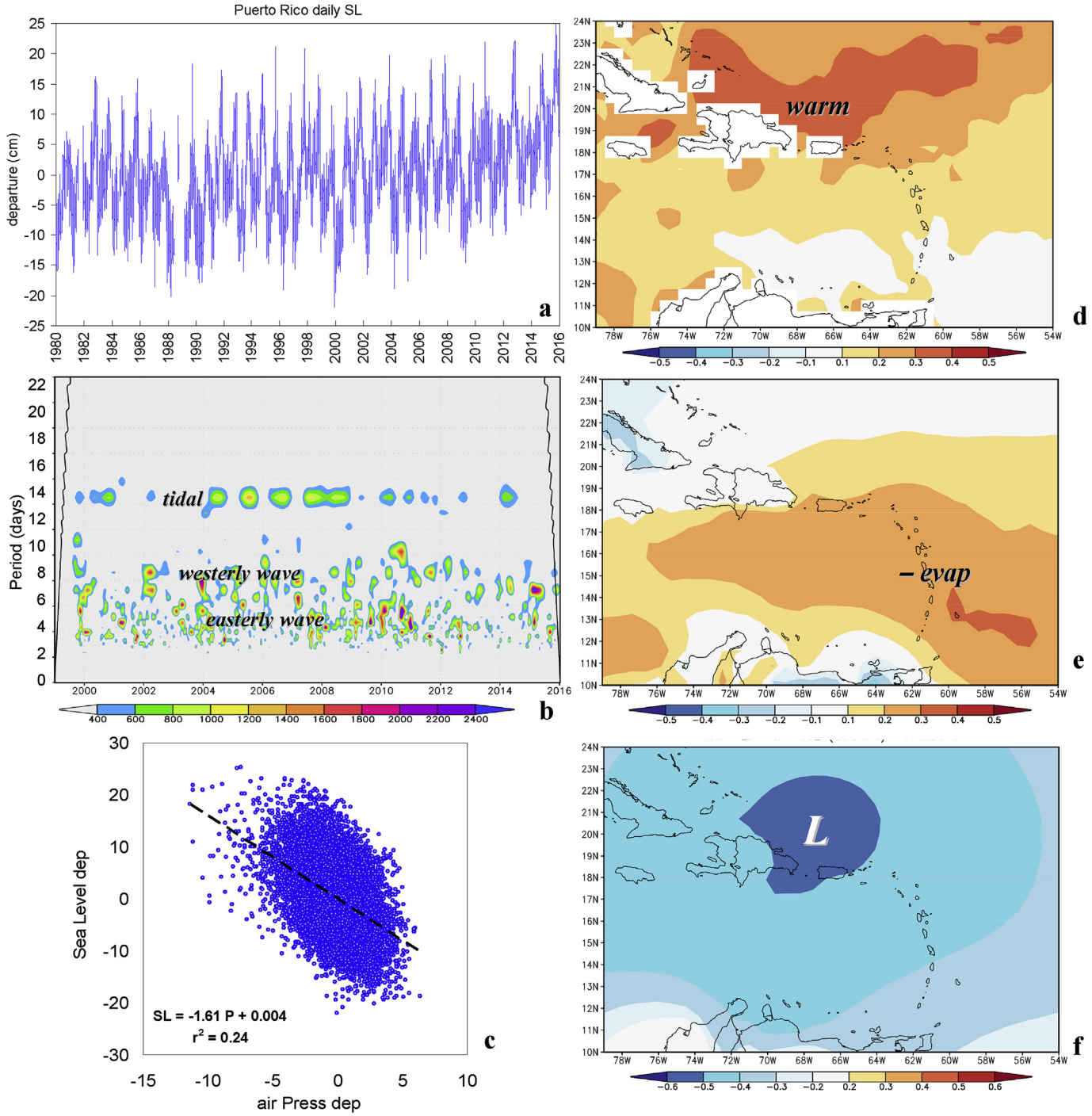

Fig. 4. (a) Time series of daily SL 1980–2015 (with 1% gaps), (b) wavelet spectra analysis of high-frequency SL since 1999; (c) scatterplot of daily SL vs local air pressure. Point-to-field regression of daily SL record 1999–2015 onto fields of: (d) SST, (e) evaporation, and (f) SLP; (correlation fraction, N = 5980).

Appendix

Photo of coastal impacts of sea level rise in Rincon, Puerto Rico (circa 2017). There was a sandy beach > 20 m wide in the (left) foreground in 2005.

References

Alfonso-Sosa, E., 2016. Sea Level Rise Detected in the Atlantic and Caribbean Coast of Puerto Rico. Ocean Physics Education. Technical Report. accessed April 2018. www.researchgate.net/publication/311557765.

Alvera-Azcárate, A., Barth, A., Weisberg, R.H., 2009. The surface circulation of the Caribbean Sea and the Gulf of Mexico as inferred from satellite altimetry. J. Phys. Oceanogr. 39, 640–657.

Andrade, C.A., Barton, E.D., 2000. Eddy development and motion in the Caribbean Sea. J. Geophys. Res. 105, 26191–26201.

Baart, F., VanKoningsveld, M., Stive, M., 2011. Trends in sea-level trend analysis. J. Coast. Res. 28, 311–315.

Boon, J.D., 2012. Evidence of sea level acceleration at US and Canadian tide stations, Atlantic coast, North America. J. Coast. Res. 28, 1437–1445.

Booth, B.B., Dunstone, N.J., Halloran, P.R., Andrews, T., Bellouin, N., 2012. Aerosols implicated as a prime driver of twentieth-century North Atlantic climate variability. Nature 484, 228–232.

Caricoos, 2018. Sea Level Rise Viewer. accessed April 2018. www.caricoos.org/sea-level-rise.

CDIAC, Carbon Dioxide Information Analysis Center. 2017. data accessed: < cdiac.ess-dive.lbl.gov/# > .

Chambers, D.P., Merrifield, M.A., Nerem, R.S., 2012. Is there a 60-year oscillation in global mean sea level? Geophys. Res. Lett. 39, L18607. https://doi.org/10.1029/2012GL052885.

Church, J.A., White, N.J., 2011. Sea-level rise from the late 19th to the early 21st century. Surv. Geophys. 32, 585–602.

Clark, J.R., 1997. Coastal zone management for the new century. Ocean Coast. Manag. 37, 191–216.

Cleveland, W.S., Devlin, S.J., 1988. Locally-weighted regression: an approach to regression analysis by local fitting. J. Am. Stat. Assoc. 83, 596–610.

Collins, W.J., co-authors, 2011. Development and evaluation of an earth-system model – HadGEM2. Geosci. Model Dev. 4, 1051–1075.

Ezer, T., Corlett, W.B., 2012. Is sea level rise accelerating in the Chesapeake Bay? A demonstration of a novel new approach for analyzing sea level data. Geophys. Res. Lett. 39, L19605. https://doi.org/10.1029/2012GL053435.

Ezer, T., Atkinson, L.P., Corlett, W.B., Blanco, J.L., 2013. Gulf Stream's induced sea level rise and variability along the US mid-Atlantic coast. J. Geophys. Res. Oceans 118, 685–697.

Frajka-Williams, E., Beaulieu, C., Duchez, A., 2017. Emerging negative Atlantic Multidecadal Oscillation index in spite of warm subtropics. Sci. Rep. 7, 11224. https://doi.org/10.1038/s41598-017-11046-x.

Fratantoni, D.M., 2001. North Atlantic surface circulation during the 1990's observed with satellite-tracked drifters. J. Geophys. Res. 106, 22067–22093.

Gyory, J., Mariano, A.J., Ryan, E.H., 2005. The Caribbean Current. RSMAS website: oceancurrents.rsmas.miami.edu/caribbean/caribbean.html.

Hamlington, B., Leben, R., Nerem, R., Han, W., Kim, K.-Y., 2011. Reconstructing sea level using cyclostationary empirical orthogonal functions. J. Geophys. Res. 116, C12015. https://doi.org/10.1029/2011JC007529.

Hernandez-Guerra, A., Joyce, T.M., 2000. Water masses and circulation in the surface layers of the Caribbean at 66°W. Geophys. Res. Lett. 27, 3497–3500.

Hu, A., Meehl, G.A., Han, W., Yin, J., 2011. Effect of the potential melting of the Greenland Ice sheet on the meridional overturning circulation and global climate in the future. Deep Sea Res. II 58, 1914–1926.

Huang, J.C.K., 1997. Climate change and integrated coastal management: a challenge for small island nations. Ocean Coast. Manag. 37, 95–107.

IPCC, 2013. Climate Change: the Physical Science Basis. Contribution of Working Group I to AR5. Cambridge University Press, UK 1535 pp.

IPCC (Intergovernmental Panel on Climate Change), 2007. Small islands: impacts, adaptation and vulnerability. In: Chapter 16, Contribution of Working Group II to AR4. Cambridge University Press, UK, pp. 687–716.

Johns, W.E., Townsend, T.L., Fratantoni, D.M., Wilson, W.D., 2002. On the Atlantic inflow to the Caribbean Sea. Deep-Sea Res. 49, 211–243.

Jury, M.R., 2015. Climatic trends in Puerto Rico observed and projected since 1980. Clim. Res. 66, 113–123.

Kenigson, J.S., Han, W., 2014. Detecting and understanding the accelerated sea level rise along the east coast of the United States during recent decades. J. Geophys. Res. Oceans 119, 8749–8766.

Klein, R.J.T., Nicholls, R.J., 1999. Assessment of coastal vulnerability to climate change. Ambio 28, 182–187.

Knudsen, M.F., Jacobsen, B.H., Seidenkrantz, M.-S., Olsen, J., 2014. Evidence for external forcing of the Atlantic multidecadal oscillation since termination of the little ice age. Nat. Commun. 5, 3323. https://doi.org/10.1038/ncomms4323.

Kopp, R.E., 2013. Does the mid-Atlantic United States sea level acceleration hot spot reflect ocean dynamic variability? Geophys. Res. Lett. 40, 3981–3985.

Lee, H.-T., Gruber, A., Ellingson, R.G., Laszlo, I., 2007. Development of the HIRS outgoing longwave radiation climate dataset. J. Atmos. Ocean. Technol. 24, 2029–2047.

Liu, Z., 2012. Dynamics of interdecadal climate variability: a historical perspective. J. Clim. 25, 1963–1995.

Molod, A., Takacs, L., Suarez, M., Bacmeister, J., 2015. Development of the GEOS-5 atmospheric general circulation model: evolution from MERRA to MERRA2. Geosci. Model Dev. 8, 1339–1356.

Murphy, S.J., Hurlburt, H.E., O'Brien, J.J., 1999. The connectivity of eddy variability in the Caribbean Sea, the Gulf of Mexico, and the Atlantic ocean. J. Geophys. Res. 104, 1431–1453.

Nicholls, R.J., 1998. Coastal Vulnerability Assessment for Sea-level Rise: Evaluation and Selection of Methodologies for Implementation. CPACC Project Report, Barbados. www.cpacc.org/download/c6assess.pdf.

NODC, National Ocean Data Center. 2017. data accessed May 2017 ≤www.nodc.noaa.gov/OC5/3M_HEAT_CONTENT/.

NSIDC, National Snow & Ice Data Center. 2017. polar ice data accessed May 2017 < nsidc.org/data/ > .
Penny, S.G., Behringer, D.W., Carton, J.A., Kalnay, E., 2015. A hybrid global ocean data assimilation system at NCEP. Mon. Weather Rev. 143, 4660–4677.
Potter, B., 1996. Tourism and Coastal Resources Degradation in the Wider Caribbean. Island Resources Foundation, St. Thomas, Virgin Islands accessed August 2016. www.irf.org/irtourdg.html.
Permanent Service for Mean Sea Level (PSMSL), 2013. Permanent Service for Mean Sea Level Tide Gauge Data. accessed August 2016. www.psmsl.org/data/obtaining/reference.php.
Reynolds, R.W., Smith, T.M., Liu, C., Chelton, D.B., Casey, K.S., Schlax, M.G., 2007. Daily high-resolution blended analyses for sea surface temperature. J. Clim. 20, 5473–5496.
Rienecker, M.M., coauthors, 2011. MERRA: NASA's modern-era retrospective analysis for research and applications. J. Clim. 24, 3624–3648.
Sallenger, A.H., Doran, K.S., Howd, P.A., 2012. Hotspot of accelerated sea-level rise on the Atlantic coast of North America. Nat. Clim. Change 2, 884–888.
Scafetta, N., 2013. Multi-scale dynamical analysis (MSDA) of sea level records versus PDO, AMO, and NAO indexes. Clim. Dynam. 43, 175–192.
Thieler, E.R., Rodriguez, R.W., Himmelstoss, E.A., 2007. Historical Shoreline Changes at Rincon, Puerto Rico, 1936-2006. USGS survey report, Woods Hole 32 pp.
Trouet, V., VanOldenborgh, G.J., 2013. KNMI Climate Explorer: a web-based research tool for high-resolution paleo-climatology. Tree-Ring Res. 69 (1), 3–13.
Turner, R., 2015. Travel and Tourism Economic Impact [in the] Caribbean. accessed August 2016. www.wttc.org/-/media/files/reports/economic%20impact%20research/regional%202015/caribbean2015.pdf.
United Nations data. 2016. accessed May 2017 < data.un.org/Data.aspx?d=PopDiv&f=variableID%3A14 > .
VanVuuren, D.P., co-authors, 2011. The representative concentration pathways: an overview. Climatic Change 109, 5–31.
Wajsowicz, R.C., 2002. A modified Sverdrup model of the Atlantic and Caribbean circulation. J. Phys. Oceanogr. 32, 973–993.
WOA (World Ocean Atlas), Locarnini, R.A., co-authors, 2013. In: In: Levitus, S. (Ed.), Temperature, vol. 1 NOAA Atlas NESDIS 73, Washington DC, USA 40 pp.
Yin, J., Schlesinger, M.E., Stouffer, R.J., 2009. Model projections of rapid sea-level rise on the northeast coast of the United States. Nat. Geosci. 2, 262–266.
Zhang, R., co-authors, 2013. Have aerosols caused the observed Atlantic multidecadal variability? J. Atmos. Sci. 70, 1135–1144.